J. KOSAE Vol. 23, No. E 1 (2007) pp. 16~28
Journal of Korean Society for Atmospheric Environment

Development of Photo-Fenton Method for Gaseous Peroxides Determination and Field Observations in Gwangju, South Korea

Wonil Chang, Jaebum Shim[1], Sangbum Hong[1] and Jai H. Lee[1],*

Department of Earth and Environmental Sciences, Korea University, 1, 5-Ga, Anam-Dong, Sungbuk-Gu, Seoul, South Korea

[1]Department of Environmental Science and Engineering, Gwangju Institute of Science and Technology, 1 Oryong-Dong, Buk-Gu, Gwangju, South Korea

(Received 27 April 2007, accepted 25 July 2007)

Abstract

An improved method was developed to determine gas-phase hydrogen peroxide (H_2O_2) and organic hydroperoxides (ROOH) in real-time. The analytical system for H_2O_2 is based on formation of hydroxybenzoic acid (OHBA), a strong fluorescent compound. OHBA is formed by a sequence of reactions, photoreduction of Fe (III)-EDTA to Fe (II)-EDTA, the Fenton reaction of Fe(II)-EDTA with H_2O_2, and hydroxylation of benzoic acid. By use of this analytical method rather than a previous similar method, Fenton reaction time was reduced from 2 min. to 30 s. Air samples were collected by a surfaceless inlet to prevent inlet line losses. With a special arrangement of the sampling apparatus, sample delivery time was drastically reduced from ~5 min to ~20 s. The automated system was found to be sensitive, capable of continuous monitoring, and affordable to operate. A comparison of this method with a well-established one showed an excellent linear correlation, validating applicability of this technique to H_2O_2 determination. The system was applied to field measurements conducted during summertime of 2004 in Gwangju, South Korea. H_2O_2 was found to be a predominant species of peroxides. The diurnal variation of H_2O_2 displayed the maximum in early afternoon and the broad minimum throughout night. H_2O_2 was correlated positively with ozone, photochemical age, and temperature, however, negatively with NO_x and relative humidity.

Key words : Hydrogen peroxide, Organic hydroperoxides, Photo-Fenton reaction, Instrumentation, Field measurements

1. INTRODUCTION

Hydrogen peroxide (H_2O_2) and organic hydroperoxides (ROOH) play important roles in atmospheric chemistry. These species are closely associated with the atmospheric oxidation capacity, the power of "cleansing" pollutants in the atmosphere (Thompson, 1992; Crutzen and Zimmermann, 1991). Gas-phase peroxides are also intimately involved in the cycling of odd-hydrogen (HO_x) radicals. Depending on the strength of production and loss processes, peroxides can serve as reservoirs of HO_x and regulate their concentrations (Kleinman, 1991; Kleinman,

* Corresponding author. Tel : +82-62-970-2444
Fax : +82-62-970-2434, E-mail : jai_h_lee@yahoo.com

1986; Logan *et al.*, 1981). Due to this close relationship with HO_x radicals, peroxides have been frequently used as a tool for validating photochemical models (Chang *et al.*, 2004; Jacob *et al.*, 1996).

H_2O_2 is known as a primary oxidant in atmospheric hydrometeors. Once dissolved in the droplets, it converts SO_2 to sulfuric acid at $pH < 4.5$ (Calvert *et al.*, 1985; Kunen *et al.*, 1983; Martin and Damschen, 1981), resulting in acidic precipitation and non-seasalt sulfate formation.

In addition, due to the much higher solubility of H_2O_2 than that of CH_3OOH, the ratio of H_2O_2 to CH_3OOH was utilized as a tracer to fingerprint recent convection, accompanied with precipitation or in-cloud reactions (Chang *et al.*, 2004; O'Sullivan *et al.*, 1999; Heikes *et al.*, 1996). Such a tracer was found to be useful to define the efficacy of heterogeneous processes in atmospheric removal of soluble gases (Chang *et al.*, 2004; O'Sullivan *et al.*, 1999; Heikes *et al.*, 1996).

Furthermore, H_2O_2 has been frequently employed as a key photochemical indicator species assessing whether the ozone production is limited by NO_x or volatile organic compounds (VOCs) (Kleinman, 2000; Sillman, 1995). For instance, a very high ratio of H_2O_2 to HNO_3 indicates NO_x-limited photochemical environment.

A number of methods have been developed to measure gaseous peroxides. Spectroscopic methods have been used in several studies. However, the majority of methods are based on collection of gaseous peroxides in aqueous solution, followed by various types of chemical analyses (Lee *et al.*, 2000). The authors provided a comprehensive review of the sampling techniques as well as the analytical methods (references therein). For the collection of gas-phase peroxides, diverse sampling methods have been developed by employing devices such as impinger, cryogenic trap, membrane diffusion scrubber, and scrubbing glass coil. Of theses methods, the scrubbing glass coil (Lazrus *et al.*, 1986) is preferred particularly for in situ field sampling due to its higher collection efficiency, little interference, and shorter collection time. The analytical determination of peroxides includes colorimetric techniques, chemiluminescence methods using luminol or peroxyoxalate, enzyme catalyzed fluorescence techniques with high performance liquid chromatography (HPLC), non-enzyme fluorescence techniques, and Fenton method. These methods have their own strengths and weaknesses as described in the earlier works (Lee *et al.*, 2000; Lee *et al.*, 1994).

Motivation of this study was to implement the weaknesses found in sampling and analytical methods in the previous studies and to develop an instrument appropriate for continuous determination of H_2O_2 and ROOH in field studies.

Lee *et al.* (1991) pointed out that significant amount of gaseous H_2O_2 could be lost by surface reactions occurring at the inlet part of the sampling line. To accurately measure gaseous peroxides, therefore, it is of critical importance to avoid this heterogeneous loss of gas-phase peroxides in the long sampling line. And thus, following Lee *et al.* (1991), the surfaceless inlet, (an inlet port without using a sampling tube) was implemented in the sampling system.

For determination of H_2O_2, several previous studies (Weinstein-Lloyd *et al.*, 1998; Lee *et al.*, 1994; Lee *et al.*, 1991; Lee *et al.*, 1990) utilized an analytical method, based on the Fenton reaction where ferrous ion (Fe(II)) reacts with H_2O_2 to produce the hydroxyl radical (OH) (R1). Benzoic acid (BA, C_6H_5COOH), in turn, scavenges OH rapidly to yield isomeric hydroxybenzoic acid (OHBA, $C_6H_5(OH)COOH$), a strong fluorescence-emitting compound (Klein *et al.*, 1975) (R2). The two reactions are expressed as follows:

$$Fe(II) + H_2O_2 \rightarrow Fe(III) + OH^- + OH \qquad (R1)$$

$$OH + C_6H_5COOH \rightarrow C_6H_5(OH)COOH \qquad (R2)$$

A reaction (R1) is slow with a rate constant of 57.8 $M^{-1}\ s^{-1}$ (Lee *et al.*, 1990). In contrast, (R2) is extremely fast and almost diffusion controlled at $4.3 \times 10^9\ M^{-1}\ s^{-1}$ (Lee *et al.*, 1990). Therefore, the yields of OH and OHBA, and the resulting fluorescence intensity are limited by (R1). In order to enhance the slow reaction rate of (R1) in the conventional Fenton method, we developed an improved analyti-

cal scheme on the basis of the fact that production of hydroxyl radical could be significantly elevated by photochemical reduction of Fe (III) to Fe (II) (Bauer *et al.*, 1999; Sun and Pignatello, 1993; Zepp *et al.*, 1992).

$$\text{Fe (III)-EDTA} + h\nu \longrightarrow \text{Fe (II)-EDTA} \quad \text{(R3)}$$

$$\text{Fe (II)-EDTA} + H_2O_2 \longrightarrow \text{Fe (III)-EDTA} + OH^- + OH \quad \text{(R4)}$$

$$OH + C_6H_5COOH \longrightarrow C_6H_5(OH)COOH \quad \text{(R2)}$$

When Fe (II)-EDTA was used instead of Fe (II) in combination with photocatalysis, as shown in (R3) and (R4), the hydroxyl radical production rate was found to be significantly increased owing to the approximately 300 times faster rate constant of (R4) ($\sim 2 \times 10^4$ M^{-1} s^{-1}) than that of (R1) (Rush and Koppenol, 1986; Bull *et al.*, 1983; Borggaard *et al.*, 1971). Consequently, since more hydroxyl radical and OHBA were produced over given time span by the increased reaction rate, it was possible to reduce retention time in the analytical system and to obtain stronger signals over narrower wavelength band in the fluorescence detector. In addition, for a reagent of the Fenton reaction, the previous studies (Lee *et al.*, 1990) used ferrous sulfate solution that was stable only below pH 2.5. In this study, however, we used Fe (III)-EDTA solution that was stable in the wider range of pH.

Compared to the conventional Fenton method (Weinstein-Lloyd *et al.*, 1998; Lee *et al.*, 1994; Lee *et al.*, 1991; Lee *et al.*, 1990), another significant improvement was made in terms of sample delivery time. With a special arrangement of the sampling apparatus, the sample delivery time was reduced from ~5 min. (Weinstein-Lloyd *et al.*, 1998; Lee *et al.*, 1994; Lee *et al.*, 1991; Lee *et al.*, 1990; Lazrus *et al.*, 1986) to ~20 s by at least an order of magnitude. This shortened sample delivery time give rise to the shorter time resolution of the instrument, making it suitable for in-situ monitoring of gaseous peroxides.

In this paper, first, we describe the instrumentation of an improved Fenton technique for in situ determination of H_2O_2. Secondly, to demonstrate that the method is responsive and affordable to operate, and therefore suitable for real-time measurements of H_2O_2 and ROOH, we deployed the instrument in a field study, conducted in Gwangju, South Korea. We present the observational results.

2. EXPERIMENTAL

The instrument was based on a dual-channel flow system where each channel was equipped with its own sampling and analytical systems; the first channel for total soluble peroxide (H_2O_2+ROOH) and the second for H_2O_2. The total peroxide was determined by a well-established method that uses p-hydroxyphenylacetic acid (pOHPAA) and horseradish peroxidase (HRP) (hereafter pOHPAA-HRP method) (Lee *et al.*, 1993; Lazrus *et al.*, 1986; Lazrus *et al.*, 1985). The concentration of H_2O_2 was obtained by the photo-Fenton method. The ROOH concentration was determined by the difference between the total soluble peroxide and H_2O_2. Since the detailed descriptions of pOHPAA-HRP method can be found in literature (Lee *et al.*, 1994), this paper focuses only on the photo-Fenton method. The schematic diagram of the photo-Fenton method is illustrated in Fig. 1.

2.1 Sampling system

The air sampling system was composed of three apparatuses (i.e., an air inlet part, a scrubbing glass coil, and an air/liquid separator). This system was originally developed by Lazrus *et al.* (1986) and then, it was improved by adding the surfaceless inlet (Lee *et al.*, 1994). The sample inlet part and the air scrubbing coil were mounted on the roof of a mobile laboratory (6 m above ground level).

Ambient air was drawn at a rate of 2 L min^{-1} by a vacuum pump through a small air inlet (1.6 mm i.d.). Concurrently, scrubbing solution (i.e., purified water) was also introduced to the sample inlet part through the port 1 (P1) at a rate of 0.3 mL min^{-1}. Gaseous peroxides were stripped from the sampled air by the scrubbing solution as passing through a 10-turn scrubbing glass coils (2 mm i.d., 120 cm in

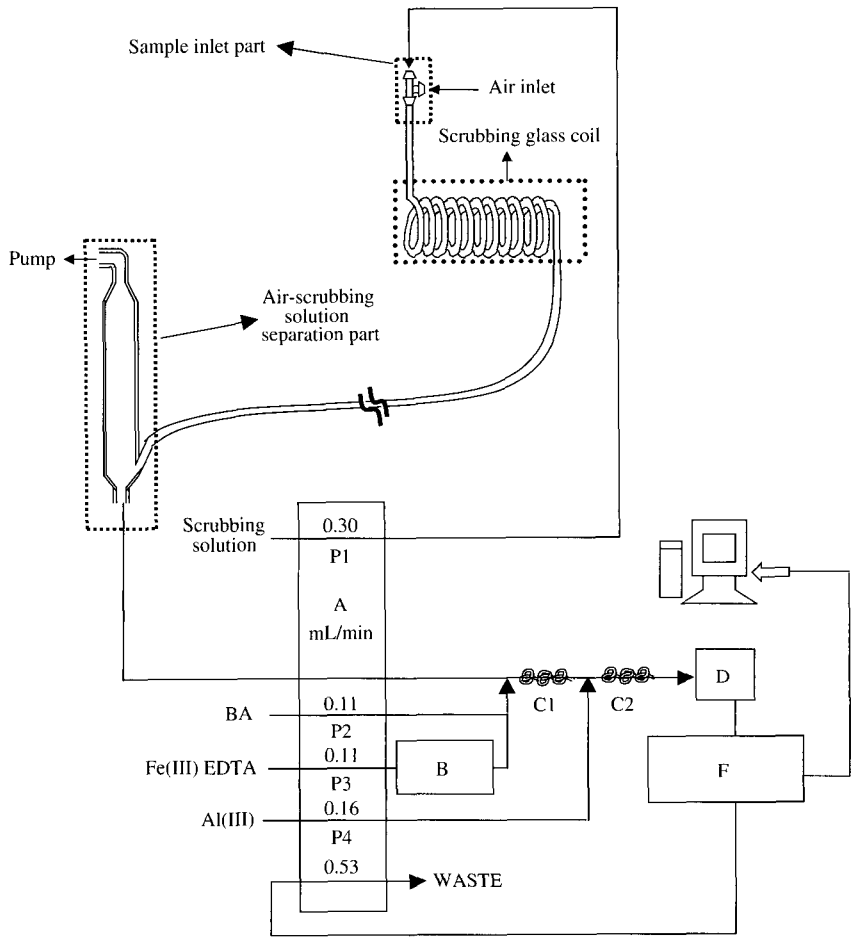

Fig. 1. A schematic diagram of the sampling and analytical systems: A: vacuum air pump; B: photoreduction chamber; C1: coil reactor where Fenton reaction occurs; C2: coil reactor where H_2O_2 sample and all reagents are mixed; D: glass debubbler; F: fluorometer; M: mass flow controller; P: peristaltic pump; P1, P2, P3, and P4 denote inlet ports delievering scrubbing solution, benzoic acid (BA) reagent, Fe (III)-EDTA reagent, and Al (III) reagent, respectively. The flow rates of the ports in mL/min are also given just above the schematic port lines.

total length). In the previous studies (Weinstein-Lloyd *et al.*, 1998; Lee *et al.*, 1994; Lee *et al.*, 1991; Lee *et al.*, 1990; Lazrus *et al.*, 1986), the separation of air from liquid was made in an air/liquid separator that was placed outside of a mobile laboratory. Then, the separated liquid was pulled via a Teflon tube into the main channel stream by a peristaltic pump. In contrast, in this work, an air/liquid separator, connected to the glass coil with a Teflon tube (3.175 mm i.d., 2 m length), was placed inside of the mobile laboratory. A mixture of air and liquid was pumped by the vacuum pump and separated in the air/liquid separator. Since the vacuum pump can transport samples much faster than the peristaltic pump, this arrangement made it possible to drastically reduce sample delivery time from ~5 min. in the earlier works (Weinstein-Lloyd *et al.*, 1998; Lee *et al.*, 1994; Lee *et al.*, 1991; Lee *et al.*, 1990; Lazrus *et al.*, 1986) to ~20 s by a factor of 15. This reduced delivery time significantly enhanced the time resolution of the instrument and thus made it appropriate to continuously measure gaseous per-

oxides in field experiments.

2.2 Analytical system

After the separation, reagent solutions were added to the liquid stream by means of a multi-channel peristaltic pump (IPC-N-16, V2.03, Ismatec Co.) through PTFE tubing (Cole-Parmer, 1.067 mm i.d.). Four inlet ports were used for H_2O_2 sample, Fe (III)-EDTA reagent, benzoic acid reagent, and fluorescence enhancing reagent (Al(III)). Through the port 1 (P1), the H_2O_2 sample or the scrubbing solution was delivered at a rate of 0.3 mL min^{-1}. The Fe(III)-EDTA solution was transferred to the photoreduction chamber (B) through the port 3 (P3) at a flow rate of 0.11 mL min^{-1}. The chamber was equipped with a 4 W low pressure Hg lamp (λ_{max}=254 nm, Philips) that photoreduced Fe (III)-EDTA to Fe (II)-EDTA by UV irradiation, as shown in (R3). The BA solution, passing through the port 2 (P2) at a flow rate of 0.11 mL min^{-1}, was merged with the Fe (II)-EDTA stream. And then, the mixed solution, containing BA and Fe (II)-EDTA, was incorporated with the H_2O_2 sample stream, entering a quartz coil-type reactor (C1). In the reactor, the Fenton-type reaction between H_2O_2 and Fe (II)-EDTA (R4) produced hydoxyl radical, which was, in turn, scavenged by BA to form OHBA (R2). Finally, before entering the second reactor (C2), the fluorescence enhancing reagent (Al(III)) was added to the main stream via the port 4 (P4) at a flow rate of 0.16 mL min^{-1} to generate the maximum level of OHBA fluorescence intensity (Lee *et al.*, 1994). Air bubbles were removed by a debubbler (D) prior to the entry to fluorometer (F) in order to prevent noisy signals by air bubbles (Martin *et al.*, 1984). The fluorescence intensity was monitored with a fluorescence detector (GTI/Spectro Vision FD-100, Groton Technology Inc., Massachusetts), equipped with an excitation filter (λ_{ex}=300 nm (CVI LASER, LLC; FWHM, 25 nm; Part#, F25-300.0-3-1.00)) and a 400-nm cutoff filter (CVI LASER, LLC; Part#, LPF-400-1.00). A 10 W Xenon flash lamp for the detector was used as a light source due to its strong output over the UV wavelength range between 225 and 350 nm. Measurement data were collected at a 1 Hz frequency using the Autochro Data Module (Young Lin, Korea).

2.3 Materials

All reagent and standard solutions were prepared with high-purity water (> 18.2 MΩ cm) from Milipore ultra-purification system. All chemicals used in this study were of reagent-grade. For the scrubbing solution, the purified water was used in both of the photo-Fenton and pOHPAA-HRP methods. The fluorescence reagent was composed of 6.8 mM pOHPAA (Sigma Chemical) and 10 units mL^{-1} horseradish peroxidase (Sigma Chemical, Type VI, P8375) in 0.085 M potassium hydrogen phthalate buffer (Sigma ACS reagent 99.99%), adjusted to pH 5.8 with 2 N NaOH (Sigma-Aldrich Chemical). In the photo-Fenton method, the fluorescence reagent contained 1.5 mM Fe (III)-EDTA (Sigma Chemical) dissolved in water and adjusted to pH 2.5 with 1 M H_2SO_4 and 2 mM Benzoic acid (Sigma Chemical). In order to enhance fluorescence, as explained by Lee *et al.* (1994), 6 mM aluminum nitrate nonahydrate ($Al(NO_3)_3 \cdot 9H_2O$, Aldrich Chemical) was prepared in 0.1 M acetate buffer adjusted to pH 3.8. The standard solutions of aqueous hydrogen peroxide were prepared from 3% H_2O_2 that had been titrated against $KMnO_4$ before calibration (Lee *et al.*, 1994).

3. RESULTS AND DISCUSSION

3.1 Optimization of analytical system

In this study, the output of the analytical system (i.e., fluorescence signal intensity) was found to be dependent on several experimental conditions or parameters such as pH, reaction time of Fe (III)-EDTA reagent, photoreduction time, and concentrations and mixing time of BA and Al (III) reagents. The analytical methodology was optimized for the best performance by adjusting and modifying these parameters.

Fig. 2a shows the variation of fluorescence signal with reaction time for (R4) followed by (R2) at three different Fe (III)-EDTA concentrations, 0.5, 1.0, and 1.5 mM, respectively. At 1.5 mM of Fe (III)-

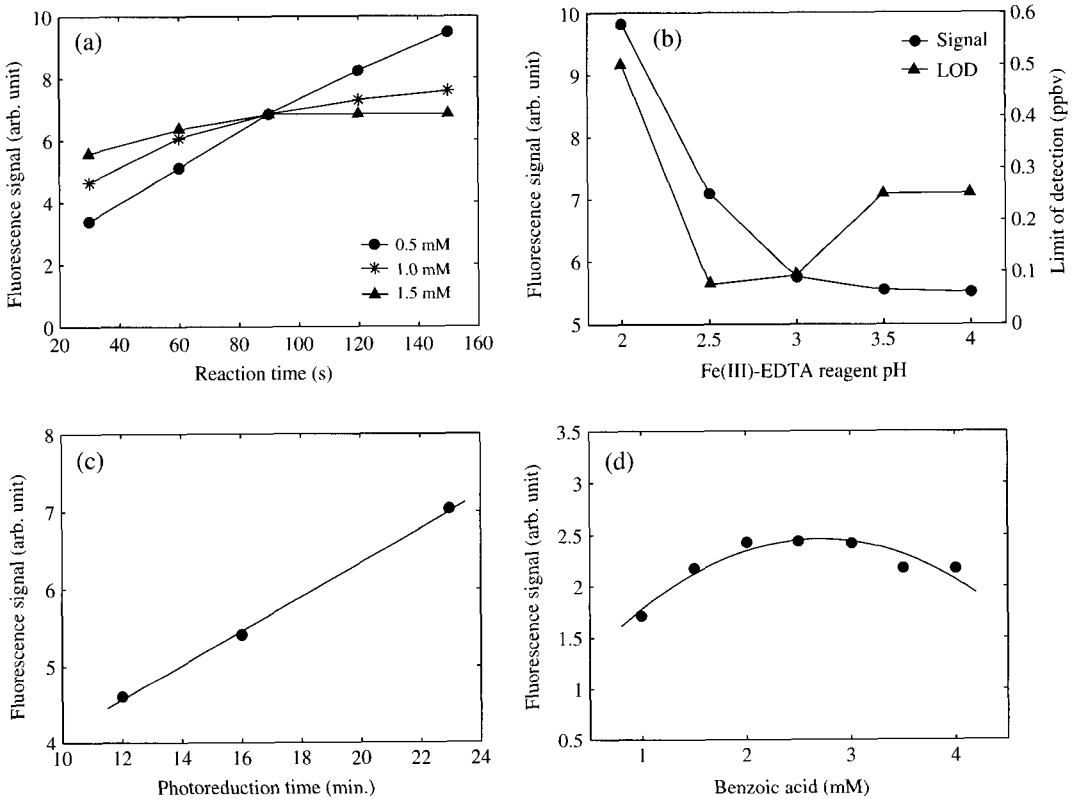

Fig. 2. Dependence of the fluorescence signal on (a) dependence of fluorescence signals on reaction time for (R4) followed by (R2) at three different Fe(III)-EDTA concentrations, 0.5, 1.0, and 1.5 mM, respectively, (b) pH of Fe(III)-EDTA reagent, (c) photoreduction time, and (d) benzoic acid concentration. 2(b) also displays limit of detection (LOD) as a function of pH. All the results in the figures were obtained under the conditions specified in Table 1 except for the parameter of interest that was varied.

EDTA, the signal approached a plateau in about 30 seconds whereas at 0.5 mM of Fe (III)-EDTA, the signal increased continuously over the time span of 150 seconds. Thus, it is obvious that the signal reached a plateau more rapidly at higher Fe (III)-EDTA concentrations. These plateaus indicated the achievement of an equilibrium state in a sequence of reactions, (R3), (R4), and (R2). This result was consistent with the previous work conducted by the conventional Fenton method (Lee *et al.*, 1990). The strongest signal was observed at the lowest level of Fe (III)-EDTA. However, this enhanced sensitivity was achieved at the expense of an unreasonably long reaction time. By compromising the analysis time and sensitivity, the optimal Fe (III)-EDTA concentration and the reaction time were determined as 1.5 mM and 30 seconds, respectively. It is worthwhile to note that the reaction time was significantly reduced by the use of the photo-Fenton method rather than the conventional Fenton technique (i.e., (R1) and (R2)). For instance, a previous study carried out by Lee *et al.* (1990) required at least a 2 minutes of reaction time that is 4-times longer than the one in this study.

The fluorescence signal and the limit of detection (LOD) were presented as a function of Fe (III)-EDTA reagent pH in Fig. 2b. The signal decreased exponentially with increasing pH, starting to level off near pH 3. On the other hand, the LOD decreased drastically between pH 2.0 and 2.5, remained almost constant at its minimum between pH 2.5 and 3.0, increased again between pH 3.0 and 3.5, and then

stayed unchanged between pH 3.5 and 4.0. To balance a good sensitivity and a relatively high signal intensity, pH 2.5 was chosen as the optimum pH of Fe (III)-EDTA reagent.

The dependence of fluorescence signal on UV irradiation time in the photoreduction chamber (B) is shown in Fig. 2c. As expected from (R3), the signal intensity increased linearly with increasing photoreduction time. In this study, a 23-minutes of photoreduction time was chosen.

Fig. 2d shows the response of the fluorescence signal to benzoic acid (BA) concentration. The signals varied in an arch shape with BA concentrations between 1.0 and 4.0 mM. A broad peak was found between 2.0 and 3.0 mM of BA. 2.0 mM was selected as the optimum BA concentration.

Although not shown, the variation of fluorescence signal was examined with respect to two additional parameters. The dependence of the fluorescence signal on BA mixing time was investigated over the time period between 0 and 90 seconds. Since the signal intensity remained virtually constant over the time interval, no mixing time was provided. Finally, the influence of mixing time of Al (III) reagent on fluorescence signal was examined. The signal reached a plateau in approximately 30 seconds that was selected as the optimum value. The resulting optimum conditions for H_2O_2 detection were summarized in Table 1.

Table 1. Summary of optimum conditions.

Parameters	Values
Peak wavelength of lamp	254 nm
Photoredution time	23 min
Fe (III)-EDTA reagent pH	2.5
Fe (III)-EDTA reagent concentration	1.5 mM
Fe (III)-EDTA reagent reaction time	30 sec
Benzoic acid reagent concentration	2 mM
Benzoic acid reagent mixing time	0 sec
Al (III) reagent mixing time	30 sec

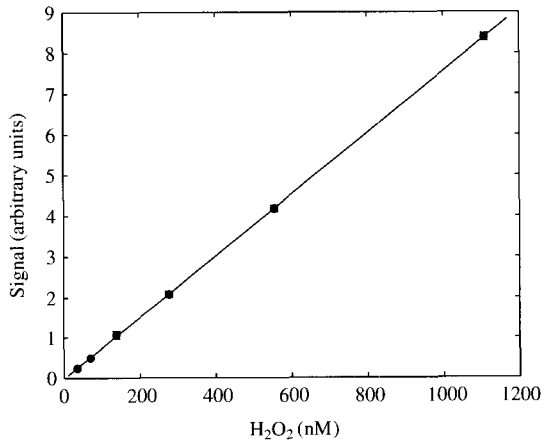

Fig. 3. Calibration curve for photo-Fenton method. Experimental conditions are given in Table 1.

3.2 Calibration and sensitivity

Under the conditions obtained from the optimization, calibration experiments were conducted by following the previous works (Lee *et al.*, 1991; Lee *et al.*, 1990). During field measurements, calibrations were carried out daily. For the calibrations, multiple standard solutions in the range of real samples were prepared by successive dilution of a stock H_2O_2 solution. And then, those were injected to the detector systems through the sample path lines. The pOHPAA-HRP channel as well as the photo-Fenton channel was simultaneously calibrated with the identical standards. As shown in Fig. 3, the calibration curve for the photo-Fenton analysis was linear with H_2O_2 concentration range between 40 and 1,100 nM. A linear regression analysis yielded an R^2 value of 0.9998. The resulting calibration curve was expressed as $y=7.57\times10^{-3}x-1.67\times10^{-2}$, where y and x denote the signal and H_2O_2 concentration, respectively. The detection limit of this technique was 10.6 nM or 39.1 pptv, based on the signal to noise ratio of 1.

3.3 Interferences

Potential interferences with various compounds were investigated in the previous studies using the Fenton-type techniques (Kwon and Lee, 2004; Lee *et al.*, 1994; Lee *et al.*, 1990). Lee *et al.* (1990) reported insignificant interferences from trace metals. Lee *et al.* (1994) did not found a substantial SO_2 interference with an exception of the encounter of SO_2 plume over the sampling site. Recently, in a ki-

netic study of HO_2^- and O_2^-, Kwon and Lee (2004) carried out extensive interference experiments by using Fe (III)-EDTA. They concluded that interferences were negligible as long as concentrations of possible inferring compounds were lower than 1 mM. It is highly unlikely to find such high equivalent concentrations of inferring compounds in gas- or aerosol-phase in ambient air.

3.4 Intercomparison between Photo-Fenton and pOHPAA-HRP Techniques

To verify an application of the photo-Fenton method to gaseous H_2O_2 determination, it was compared to the pOHPAA-HRP method, one of the well -established methods. H_2O_2 samples were collected and analyzed simultaneously by both instruments. Fig. 4 shows an excellent linear correlation between H_2O_2 concentrations determined by the photo-Fenton method and the pOHPAA-HRP method. A linear regression analysis gave a correlation coefficient of 0.998 and a slope of 1.12 with higher values for the photo-Fenton method. Therefore, this result clearly demonstrated an application of the photo-Fenton method as a promising analytical method for H_2O_2 measurement.

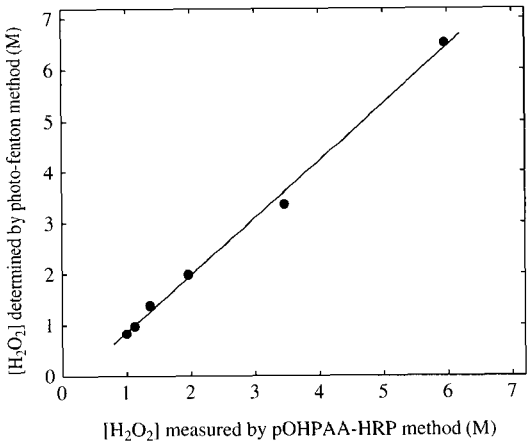

Fig. 4. Comparison of photo-Fenton and pOHPAA-HRP methods. The solid line denotes 1 : 1 line.

4. FIELD MEASUREMENTS

Using the newly developed instrument, field measurements of H_2O_2 and ROOH were made in summertime from May 23 to June 24, 2004 at GIST (Gwangju Institute of Science and Technology), Gwangju, South Korea. Other photochemical key species and physical variables were also measured simultaneously. Gwangju is one of major cities in South Korea with a population of about 1.4 million. GIST is located in the northern part of the city substantially away from the downtown pollution sources (35° 10′N and 126° 50′E).

Table 2 summarizes statistical results of H_2O_2 and ROOH measured only under the fair weather conditions. Although samples were collected and analyzed in 1 min. interval, in the table, 10-min. averaged data were presented. The time windows, correspond-

Table 2. Statistical comparisons of H_2O_2 and ROOH concentrations observed during the field measurement.

Species	No.	Mean±σ	Med.	Max.	Min.	95%	5%
			Total (00:00~24:00 hour)				
H_2O_2	1516	1.37±1.07	0.960	5.20	<LOD*	3.64	0.362
ROOH	1193	0.870±0.903	0.561	6.91	<LOD	2.54	0.0440
			Daytime (09:00~18:00 hour)				
H_2O_2	582	2.08±1.14	1.98	5.20	<LOD	4.13	0.411
ROOH	558	1.00±0.819	0.746	3.77	<LOD	2.64	0.113
			Nighttime (20:00~04:00 hour)				
H_2O_2	478	0.886±0.570	0.671	3.65	0.105	2.14	0.368
ROOH	333	0.743±1.10	0.362	6.91	<LOD	2.49	0.0230

No., σ, Med., Max., Min., 95%, and 5% denote the number of measured data, standard deviation, median, maximum, minimum, 95th percentile, and 5th percentile, respectively. <LOD* represents the concentrations of species below the limit of detection.

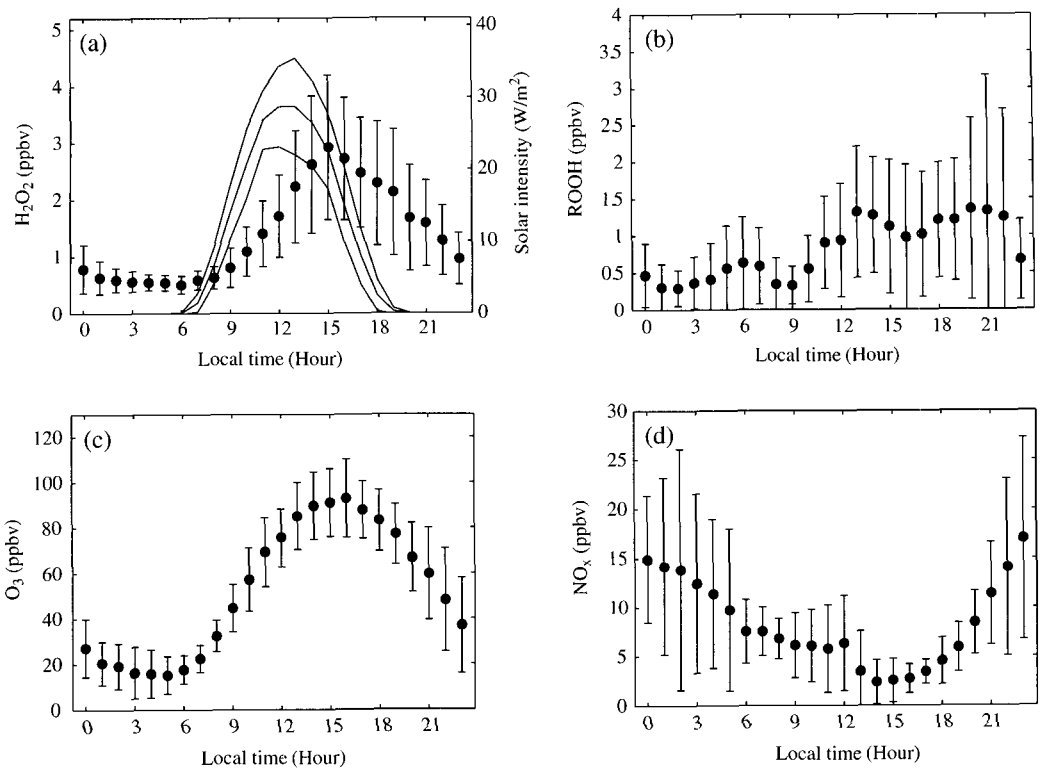

Fig. 5. Diurnal variations of (a) H_2O_2, (b) ROOH, (c) O_3, and (d) NO_x observed from May 23 to June 24, 2004. The filled circles and error bars denote the mean values (M) and one standard deviation from the means ($\pm 1\sigma$), respectively. In 5 (a), three solid lines represents solar radiation intensity, $M+\sigma$, M, $M-\sigma$ from the top to the bottom, respectively.

ing to total, daytime, and nighttime, were 00:00~24:00, 09:00~18:00, and 20:00~04:00 hours, respectively. The time windows were chosen so that local emission influence was minimized during commute hours of morning and evening. In all the time windows, H_2O_2 concentrations were higher than ROOH concentrations. Higher ratios of H_2O_2 to ROOH were found during the daytime than the nighttime. On the basis of the mean values, the ratios in nighttime were close to unity whereas those in daytime was about two. This result may reflect the faster deposition of H_2O_2 than ROOH to the surface during nighttime when surface condensation of water vapor may occur due to the elevated relative humidity and lowered temperature.

Diurnal variations of H_2O_2, ROOH, O_3, and NO_x are shown in Figs. 5a, 5b, 5c, and 5d, respectively. In theses figures, only one-hour averaged data are presented. The filled circles and error bars represent hourly means (M) and one standard deviations (σ), respectively. In Fig. 5a, solar radiation intensities are also displayed by three solid lines: $M+\sigma$, M, $M-\sigma$ from the top to the bottom, respectively. Low H_2O_2 concentrations were observed with little variation throughout the night and early morning (01:00~08:00 hours) (Fig. 5a). After 08:00 hour, however, H_2O_2 started to increase rapidly, reaching the maximum at 15:00 hour and then decreasing sharply from 15:00 to 01:00 hours. In contrast, ROOH concentrations did not show a distinctive diurnal trend although they appeared to increase from 01:00 to 21:00 hours with some fluctuations and then decreased drastically between 22:00 and 00:00 hours (Fig. 5b). The diurnal profile of O_3 was similar to that of

H_2O_2 (Fig. 5c). It is noticeable that O_3 concentrations built up starting from around sunrise (06:00 hour) whereas H_2O_2 began to escalate two hours later at 08:00 hour. The time gap between the initial increases of H_2O_2 and O_3 may indicate the requirement of about two hours in order for sufficient HO_2 (a precursor of H_2O_2) to be produced photochemically from O_3. NO_x showed a diurnal pattern opposite to those of H_2O_2 and O_3; higher in nighttime and lower in daytime (Fig. 5d). It is interesting to observe that the maximum values of H_2O_2 and O_3 and the minimum value of NO_x coincided around 15:00 hour. These coincidences and similar diurnal variations of the three species have been observed in a number of previous studies of throughout the world, conducted in Los Angeles (Sakugawa and Kaplan, 1989), Southern England (Dollard *et al.*, 1989), North Carolina (Das and Aneja, 1994), Portugal (Jackson and Hewitt, 1996), and Japan (Takami *et al.*, 2003). From these results, it is clear that H_2O_2 diurnal behavior was closely related with those of O_3 and NO_x After sunrise, O_3 start to be formed by the reaction of an oxygen molecule with O (^{3}P), a product resulting from the photolysis of NO_2. O_3, in turn, is photolyzed to form an excited oxygen atom, O (^{1}D), which reacts with water vapor to yield two OH radicals. The OH attacks CO to form HO_2 radical and the self-reaction of HO_2 leads to H_2O_2 production under the low NO_x condition. The concurrence of the diurnal maxima of H_2O_2 and O_3 and the diurnal minimum of NO_x can be explained by the fact that H_2O_2 formation favors high O_3 and low NO_x levels. Between 18:00 and 24:00 hours, the decrease in H_2O_2 can be attributed to dry and/or wet deposition due to its high solubility and lack of replenishment from the free troposphere. On the other hand, over the same period, the O_3 decrease can be ascribed to NO_x titration since NO_x concentrations increased rapidly.

Table 3 show correlations of H_2O_2 with photochemical and physical variables. It is to be noted that data used in the table were those measured in the daytime (09:00 ~ 18:00 hours) in order to investigate H_2O_2 behavior under the conditions when photochemistry was active. ROOH was not well correlated with H_2O_2 (r=0.20) although both have common precursor, HO_2, for their formations. As expected from comparison of Fig. 5a with 5c and 5d, H_2O_2 shows a strong positive correlation with O_3 (r=0.69), but a strong negative correlation with NO_x (r=−0.56). The ratio of NO_z (i.e., NO_y−NO_x) to NO_y (i.e., sum of all gas-phase nitrogen compounds) has been frequently utilized as a parameter measuring the degree of photochemical processing in an air parcel (Trainer *et al.*, 2000). H_2O_2 was strongly correlated with the NO_z/NO_y ratio (r=0.65). Therefore, this result indicates that H_2O_2 formation was favorable in photochemically well-aged airmasses. Table 3 also shows correlations between H_2O_2 and two physical variables, temperature (T) and relative humidity (RH). H_2O_2 was correlated positively with T (r=0.71) but negatively with RH (r=−0.45). This result is consistent with those observed in the previous studies where potential reasons were given (Takami *et al.*, 2003; Jackson and Hewitt, 1996; Das and Aneja, 1994; Sakugawa and Kaplan, 1989). This result also supports the lower ratio of H_2O_2 to ROOH in nighttime due to the increased surface deposition as implied above (Table 2).

Table 3. Correlations between H_2O_2 and chemical and physical variables.

Variables	ROOH	O_3	NO_x	NO_z/NO_y	T	RH
r	0.20	0.69	−0.56	0.65	0.71	−0.45

r, T, and RH denote correlation coefficient, temperature, and relative humidity. For the definition of NO_z and NO_y, refer to the text.

5. SUMMARY AND CONCLUSIONS

On the basis of photo-Fenton reactions, an improved analytical instrument was developed to measure gaseous hydrogen peroxide and organic hydroperoxides in real-time. The instrument was composed, in large, of two systems, a sampling system and an analytical system. The sampling system was implemented with the surfaceless inlet in order to avoid heterogeneous loss of H_2O_2 in the long sampling line. By the use of Fe (II)−EDTA instead of Fe (II) and the photoreduction of Fe (III)−EDTA to

Fe (II)-EDTA, the analytical system was significantly improved in terms of the reaction time and the signal strength. In addition, by reducing drastically sample delivery time, the time resolution of the analytical system was substantially improved. Therefore, theses two important improvements made this instrument suitable for continuous monitoring of gaseous peroxides. The analytical method was optimized for the best performance by adjusting experimental conditions such as pH and reaction time of Fe (III)-EDTA reagent, photoreduction time, and concentrations and mixing time of BA and Al (III) reagents. In order to verify the utility of the photo-Fenton method for gaseous H_2O_2 determination, it was compared to the pOHPAA-HRP method. The former was linearly correlated with the latter with an excellent correlation coefficient of 0.998. Therefore, these experimental results clearly demonstrated the photo-Fenton method promising for real-time atmospheric H_2O_2 determination.

The newly developed system was deployed in field study. Between H_2O_2 and ROOH, H_2O_2 was found to be the dominant species, particularly during the daytime. Higher ratio of H_2O_2 to ROOH was observed during the daytime than the nighttime, reflecting faster deposition of H_2O_2 than ROOH to the surface during nighttime. H_2O_2 exhibited a distinctive diurnal cycle with a peak at 3 PM, whereas ROOH did not. The maxima of H_2O_2 and O_3 and the minimum of NO_x coincided around 3 PM. These results were consistent with those observed earlier over the world. In investigation of correlations between H_2O_2 and photochemical and physical variables in daytime, H_2O_2 was strongly correlated with O_3, NO_x, photochemical age, temperature. However, H_2O_2 was correlated weakly with ROOH and moderately with relative humidity.

ACKNOWLEDGEMENTS

This work was supported by the Korea Research Foundation Grant funded by Korea Government (MOEHRD, Basic Research Promotion Fund) (KRF-2005-075-c00037) and in part by the Korea Science and Engineering Foundation (KOSEF) through the Advanced Environmental Monitoring Research Center (ADEMRC) at Gwangju Institute of Science and Technology (GIST) and the Brain Korea 21 Project, Ministry of Education and Human Resources Development (MOE) Korea.

REFERENCES

Bauer, R., G. Waldner, H. Fallmann, S. Hager, M. Klare, T. Krutzler, S. Malato, and P. Maletzky (1999) The photo-fenton reaction and the TiO_2/UV process for waste water treatment-novel developments, Catalysis Today, 53, 131-144.

Borggaard, O.K., O. Farver, and V.S. Andersen (1971) Polarographic study of the rate of oxidation of iron (II) chelates by hydrogen peroxide, Acta Chem. Scand., 25, 3541-3543.

Bull, C., G.J. McClune, and J. Fee (1983) The mechanism of Fe-EDTA catalyzed superoxide dismutation, J. Am. Chem. Soc., 105, 5290-5300.

Calvert, J.C., A.L. Lazrus, G.L. Kok, B.G. Heikes, J.G. Walega, J. Lind, and C.A. Cantrell (1985) Chemical mechanisms of acid generation in the troposphere, Nature, 317, 27-35.

Chang, W., M. Lee, and B.G. Heikes (2004) One dimensional photochemical study of H_2O_2, CH_3OOH, and HCHO in the remote marine boundary layer during Pacific Exploratory Mission in the Tropics (PEM-TROPICS) B, J. Geophys. Res., 109, D06307, doi:10.1029/2003JD004256.

Crutzen, P.J and P.H. Zimmermann (1991) The changing photochemistry of the troposphere, Tellus, 43AB, 136-151.

Das, M. and V.P. Aneja (1994) Measurements and analysis of concentrations of gaseous hydrogen peroxide and related species in the rural central Piedmont region of North Carolina, Atmos. Environ., 28, 2473-2483.

Dollard, G.J., F.J. Sandalls, and R.G. Derwent (1989) Measurement of Gaseous Hydrogen Peroxide in Southern England During a Photochemical Episode, Environmental Pollution, 58, 115-124.

Heikes, B.G., M. Lee, J. Bradshaw, S. Sandholm, D. Davis, J. Crawford, J. Rodriguez, S. Liu, S. McKeen, D. Thorton, A. Bandy, G. Gregory, R.

Talbot, and D. Blake (1996) Hydrogen peroxide and methylhydroperoxide distribution related to ozone and odd hydrogen over the North Pacific in the fall of 1991, J. Geophys. Res., 101, 1891-1905.

Jackson, A.V. and C.N. Hewitt (1996) Hydrogen peroxide and organic hydroperoxide concentrations in air in a EUCALYPUS forest in central portugal, Atmospheric Environ., 30, 819-830.

Jacob, D.J., B.G. Heikes, S.-M. Fan, Logan, J., D.L. Mauzerall, J.D. Bradshaw, H.B. Singh, G.L. Greogory, R.W. Talbot, D.R. Blake, and G.W. Sachse (1996) Origin of ozone and NO_x in the tropical troposphere: A photochemical analysis of aircraft observations over the South Atlantic basin, J. Geophys. Res., 101, 24235-24250.

Klein, G.W., K. Bhatia, V. Madhavan, and R. H. Schuler (1975) Reaction of · OH with benzoic acid. isomer distribution in the radical intermediates, J. Physical Chem., 79, 1767-1774.

Kleinman, L.I. (1986) Photochemical formation of peroxides in the boundary layer, J. Geophys. Res., 91, 10889-10904.

Kleinman, L.I. (1991) Seasonal dependence of boundary layer peroxide concentration: the low and high NO_x Regimes, J. Geophys. Res., 96, 20721-20733.

Kleinman, L.I. (2000) Ozone process insights from field experiments-part II: Observation-based analysis for ozone production, Atmos. Environ., 34, 2023-2033.

Kunen, S.M., A.L. Lazrus, G.L. Kok, and B.G. Heikes (1983) Aqueous Oxidation of SO_2 by Hydrogen Peroxide, J. Geophys, Res., 88, 3671-3674.

Kwon, B.G. and J.H. Lee (2004) A Kinetic Method for HO_2 · /O_2^- · Determination in Advanced Oxidation Processes, Anal. Chem, 76, 6359-6364.

Lazrus, A.L., G.L. Kok, S.N. Gitlin, J.A. Lind, and S.E. McLaren (1985) Automated fluorometric method for hydrogen peroxide in atmospheric precipitation, Anal. Chem., 57, 917-922.

Lazrus, A.L., G.L. Kok, J.A. Lind, S.N. Gitlin, B.G. Heikes, and R.E. Shetter (1986) Automated fluorometric method for hydrogen peroxide in air, Anal. Chem, 58, 594-597.

Lee, J.H., I.N. Tang, and J.B. Weinstein-Lloyd (1990) Nonenzymatic Method for the Determination of Hydrogen Peroxide in Atmospheric Samples, Anal. Chem., 62, 2381-2384.

Lee, J.H., Y. Chen, and I.N. Tang (1991) Heterogeneous loss of gaseous H_2O_2 in an atmospheric air sampling system, Environ. Sci. Technol., 25, 339-342.

Lee, J.H., D.F. Leahy, I.N. Tang, and L. Newman (1993) Measurement and speciation of gas phase peroxides in the atmosphere, J. Geophys. Res., 98, 2911-2915.

Lee, J.H., I.N. Tang, J.B. Weinstein-Lloyd, and E.B. Halper (1994) Improved nonenzymatic method for the determination of gas-phase peroxids, Envron. Sci. Technol., 28, 1180-1185.

Lee, M., B.G. Heikes, and D.W. O'Sullivan (2000) Hydrogen peroxide and organic hydroperoxide in the troposphere: a review, Atmos. Environ., 34, 3475-3494.

Logan, J.A., M.J. Prather, S.C. Wofsy, and M.B. McElroy (1981) Tropospheric Chemistry: A Global Perspective, J. Geophys, Res., 86, 7210-7254.

Martin, L.R. and D.E. Damschen (1981) Aqueous Oxidation of Sulfur Dioxide by Hydrogen Peroxide at Low pH, Atmos. Environ., 15, 1615-1621.

Martin, G.B., H.K. Cho, and M.E Meyerhoff (1984) Tubular debubbler for segmented continuous-flow automated analyzers, Anal. Chem., 56, 2612-2613.

O'Sullivan, D.W., B.G. Heikes, M. Lee, W. Chang, G.L. Gregory, D.R. Blake, and G.W. Sachse (1999) Distribution of hydrogen peroxide and methylhydroperoxide over the Pacific and South Atlantic Oceans, J. Geophys. Res., 104, 5635-5646.

Rush, J.D. and W.H. Koppenol (1986) Oxidizing Intermediates in the Reaction of Ferrous EDTA with Hydrogen Peroxide, The Journal of Biological Chemistry, 261, 6730-6733.

Sakugawa, H. and I.R. Kaplan (1989) H_2O_2 and O_3 in the atmosphere of Los Angeles and its vicinity: factors controlling their formation and their roles as oxidants of SO_2, J. Geophys, Res., 94, 12957-12973.

Sillman, S. (1995) The use of NO_y, H_2O_2, and HNO_3 as indicators for ozone-NO_x-hydrocarbon sensitivity in urban locations, J. Geophys. Res., 100, 14175-14188.

Sun, Y. and J.J. Pignatello (1993) Photochemical reactions involved in the total mineralization of 2, 4-D by iron (3+)/hydrogen peroxide/UV, Environ. Sci.

Technol, 27, 304-310.

Takami, A., N. Shiratori, H. Yonekura, and S. Hatakeyama (2003) Measurement of hydroperoxides and ozone in Oku-Nikko area, Atmos. Environ., 37, 3861-3872.

Thompson, A.M. (1992) The oxidizing capacity of the earth's atmosphere: Probable past and future change Science, 256, 1157-1165.

Trainer, M., D.D. Parrish, P.D. Goldan, J. Roberts, and F.C. Fehsenfeld (2000) Review of observation-based analysis of the regional factors influencing ozone concentrations, Atmos Environ., 34, 2045-2061.

Weinstein-Lloyd, J.B., L.J. Lee, P.H. Daum, L.I. Kleinman, L.J. Nunnermacker, and S.R. Springston (1998) Measurements of peroxides and related species during the 1995 summer intensive of the Southern Oxidants Study in Nashville, Tennessee, J. Geophys. Res., 103, 22361-22373.

Zepp, R.G., B.C. Faust, and J. Hoigne (1992) Hydroxyl radical formation in aqueous reactions (pH 3~8) of iron (II) with hydrogen peroxide: the photo-Fenton reaction, Environ. Sci. Technol., 26, 313-319.